Available online at www.sciencedirect.com
SCIENCE DIRECT®
Journal of Photochemistry and Photobiology A: Chemistry 173 (2005) 156–160
Journal of Photochemistry and Photobiology A:Chemistry
www.elsevier.com/locate/jphotochem

# Nanoparticle mediated photodefluorination monitored by $^{19}$F NMR

Joyce Chow, Nin N. Dingra, Elizabeth Baker, Brian C. Helmly, Delana A. Nivens *, Will E. Lynch

*Department of Chemistry and Physics, Armstrong Atlantic State University, Savannah, Georgia 31419, USA*

Received 23 August 2004; received in revised form 26 January 2005; accepted 27 January 2005
Available online 5 March 2005

**Abstract**

The photoreduction of monofluorinated phenols and benzoic acids on polyphosphate capped ZnS nanoparticles is examined. Defluorination is monitored using $^{19}$F NMR. Photoreductive defluorination on ZnS nanoparticles produces fluoride while direct photolysis produces ring opening products. Reaction on bulk ZnS produces ≪1% defluorination under the same conditions. The quantum yield and turnover numbers are presented for six compounds with the fluoride substituted at different positions around the aromatic ring. The reaction rates are affected by the presence of electron donating or withdrawing groups attached to the aromatic ring. The rates of product produced are 4-fluorophenol > 2-fluorophenol > 3-fluorophenol when the electron donating hydroxyl group is present and the opposite trend of 3-fluorobenzoic acid > 2-fluorobenzoic acid > 4-fluorobenzoic acid when an electron withdrawing group is attached to the benzene.


*Keywords:* Nanoparticle; Zinc sulfide; Defluorination; $^{19}$F NMR; Photoreduction; Remediation

## 1. Introduction

Ubiquitous in the environment, halogenated aromatic compounds have long been known to be environmental hazards due to their toxicity. Photocatalytic methods for degrading these compounds are widely investigated and have been reviewed in the literature [1–7]. Photooxidation of organics on $TiO_2$ has been the most widely investigated method primarily for $TiO_2$'s low cost and propensity to completely mineralize halogenated organic compounds to the less toxic products $CO_2$, mineral acid and water. This generally achieved without producing toxic intermediates often seen during direct photolysis [7–9]. More recently, nanoscale photoreactive catalysts of $TiO_2$ and other compounds such as $MoS_2$, $SnO_2$, ZnS, CdS and mixed systems have been investigated for the destruction of organic compounds [4,5,9–11]. These compounds are of interest because they allow for tuning the HOMO-LUMO transition toward the visible region of the spectrum (versus ultraviolet for bulk particles) as well as increased catalytic efficiencies with larger surface areas found in nanoparticles.

Further, spectroscopy and photocatalysis involving nanoparticles have received increased attention in the literature due to the new properties exhibited as a result of quantum confinement [4,5,10,12–20]. These quantum effects begin to appear when materials become smaller than the Bohr exciton radius, generally around 100 nm or less in diameter. The optical and catalytic properties of such compounds are dominated by quantum confinement and surface effects. Changes to smaller particle size blue shift the absorbance spectrum of the molecule and with a corresponding change in the band-gap energy to higher energy. Nano-size semi-conductor photocatalysts have been observed to be more effective than their bulk counterparts for numerous reasons including increased surface area, lower scattering, increased photostability (except CdS and CdSe) and ability to tune absorbance wavelength to allow more of the sun-spectrum to be used for photocatalysis and photoremediation [5,10,21,22].

In this paper, we examine the photodecomposition of fluorinated aromatic compounds when exposed to 290–360 nm light in the presence of polyphosphate capped, nanosized ZnS

* Corresponding author. Tel.: +1 912 921 5447; fax: +1 912 961 3226.
*E-mail address:* nivensde@mail.armstrong.edu (D.A. Nivens).

1010-6030/$ – see front matter © 2005 Elsevier B.V. All rights reserved.
doi:10.1016/j.jphotochem.2005.01.015

[19,20]. The electron is photochemically excited to the conduction band and then transferred by a surface process to the substrate. The decomposition of 2-, 3-, or 4-fluorophenol as well as 2-, 3-, or 4-fluorobenzoic acid is monitored by $^{19}F$ NMR and shows that the reduction product of the decomposition is fluoride ion. The other products of the photochemical processes are the corresponding dihydroxybenzenes for the fluorophenols whereas the fluorobenzoic acid derivatives yield the appropriate hydroxybenzoic acid or dimethylamine products generated from the corresponding oxidation of solvent water or DMF. In our experiments, a 463-fold excess of fluorinated (12.5 mM) compound to nanoparticle (27 μM) under a 24 h illumination period converts as much as 59.5% of substrate to products. This equates to a maximum turnover number of 275 as calculated by dividing the concentration of fluoride concentration per catalyst concentration. The rates of these photolysis experiments are related to the electron withdrawing/donating resonance effects of the carboxylic acid or phenol substituent. Direct photolysis of the fluorinated compounds using these wavelengths yield the products outlined above where as bulk ZnS catalyst yielded ≪1% photoreduction or a maximum turnover number of 3 over our time course.

## 2. Experimental section

### 2.1. Materials

Zinc acetate dihydrate, sodium sulfide nonahydrate, ZnS bulk powder, trichlorofluoromethane, sodium fluoride, 4-fluorophenol, 3-fluorophenol, 2-fluorophenol, 4-fluorobenzoic acid, 3-fluorobenzoic acid and 2-fluorobenzoic were purchased from Aldrich Chemical Company and used as received.

### 2.2. Equipment

The centrifuge used for purification of the ZnS nanoparticles was a Thermo IEC Centra CLE centrifuge. A Hewlett Packard 8452 UV–vis Spectrometer was used to record absorbance spectra from 190 to 1100 nm. An 100 W Xe Lamp from Oriel was used as the light source with two filters, a 300 nm long pass filter and a 310 nm band pass (20 nm) filter (Oriel) to provide light over the range of 290–360 nm with 20% transmittance at the center wavelength. The power at the sample was measured to be 6 mW/cm$^2$ using a UV-light monitor (Fisher Scientific). A JEOL Eclipse 300 MHz was used to record NMR data. $^{19}F$ NMR spectra were collected at 282.8 MHz in $H_2O$ unlocked at 22 CircC in a standard 5 mm NMR tube. The 64 transients collected, had a 0.2177 s acquisition time, 5 μs pulse and recycle delay of 4 s. The spectra were processed with a single exponential window and backwards-linear prediction (BLIP) reconstructing the first 64 points was used to remove the Teflon background signal of the probe. Product identification was made via GC–MS using a Hewlett Packard 6890 gas chromatograph coupled with a mass selective detector.

### 2.3. Nanoparticle preparation

Nanoparticles of zinc sulfide, ZnS, were prepared according to a previously published procedure [20]. All procedures were carried out in 18 MΩ deionized water. A 1.0 M solution of zinc acetate and a 0.85 M solution of sodium sulfide and were prepared in deionized water. A 10.2 g of sodium polyphosphate was placed in 80 mL of deionized water and stirred until dissolved. Ten milliliters of the zinc acetate solution was then added and vigorous stirring continued. Finally, in one portion, 10 mL of the sodium sulfide solution was added. Immediately an off-white solution was observed. Stirring was continued for a total of 2 min. The solution was then centrifuged (3500 rpm for 10 min), decanted and washed two times with deionized water with subsequent centrifuging. The final ZnS nanoparticle solution was prepared by suspending the entire solid particulate in 300 mL of deionized water. This prepared a solution of 3.6 nm ZnS nanoparticle concentration of not greater than $5.4 \times 10^{-5}$ M. The ZnS nanoparticles were stable in solution for over 6 weeks as evidenced by no observable precipitation of the particles and was used for both spectroscopic analysis as well as photocatalysis experiments without further purification.

### 2.4. Photocatalysis

Aqueous solutions of the fluorinated aromatic compounds were freshly prepared each day at 25 mM, twice the target concentration. The fluorobenzoic acid derivatives have minimal solubility in water and a 6% aqueous DMF solution was used to assist with solubility. Once prepared, fluorinated stock solutions were stored in the dark. In polyborosilicate NMR tubes, 500 μL of the fluorinated aromatic solution was combined with 500 μL of the ZnS nanoparticle solution and mixed well. An initial NMR spectrum ($t = 0$) was recorded. The NMR tube was then placed at the focal point of the Xe lamp. NMR spectra were recorded periodically for three hours and then left overnight to determine if complete conversion would occur in 24 h.

### 2.5. Actinometry

Standard oxalic acid/uranyl nitrate actinometry was performed to measure the apparent quantum yield of the reactions. A 10 mM oxalic acid was combined with 10 mM uranyl nitrate in NMR tubes in the dark and exposed to the same lamp conditions at the fluorinated compounds. A standardized potassium permanganate solution was used to titrate the oxalic acid samples. Using the accepted value of 0.57 as the quantum yield for oxalic acid decomposition, the lamp produced $1.0 \times 10^{-7}$ Einsteins/min over the wavelength range used.

## 3. Results and discussion

### 3.1. Nanoparticle characterization

The synthesis of the ZnS nanoparticles is straightforward and produces product of sufficient purity suitable for photochemical reaction studies. By examining the UV–vis spectra (Fig. 1), ZnS can be characterized to determine the band gap energy. This HOMO–LUMO transition energy coupled with the Brus equation [14], allows one to determine the particle size from known parameters. The ZnS nanoparticles initially have an absorbance maxima of 295 nm, but after aging, the absorbance is slightly red shifted (Fig. 1). From the absorption spectra of ZnS nanoparticles in this study, the energy separating the valence and conduction bands ranges from 4.20 to $3.91 \pm 0.13$ eV. This results in a calculated diameter of the particles at $3.6 \pm 0.4$ nm initially to $6.1 \pm 0.7$ nm over the course of our experiments. This value agrees well with the literature value provided for fresh ZnS nanoparticles prepared this synthetic scheme of 3.7 nm [20]. The band gap energy between the HOMO (valence band) and LUMO (conduction band) of bulk ZnS material purchased directly from the manufacturer is ~3.68 eV, resulting from a transition at 337 nm (Table 1).

### 3.2. Fluoride degradation

The photodefluorination was performed by illuminating a mixture of 12.5 mM fluorinated substrates and 27 μM ZnS nanoparticles over the wavelength range of 290–340 nm. The nanoparticle concentration was determined by relating the spectrophotometrically determined particle size to the number of equivalents of ZnS per particle. This is determined from the unit cell parameters of ZnS blende. The 3.6 nm particle size implies a volume of 24.4 $nm^3$, which contains approximately 154 unit cells of ZnS blende with $Z = 4$. Thus, 616 equivalents of ZnS are present per particle. The equivalents of ZnS can also found by considering the number of lattice planes in the 3.6 nm particle (~11) [23] or via the density of ZnS. Thus, when the amount of zinc present is divided by the total volume of 300 mL, the maximum ZnS concentration is determined to be not greater than $5.4 \times 10^{-5}$ M. Therefore, as the particle size gets larger over the time course of the reaction, the nanoparticle concentration decreases. Thus all reaction yields are reported in minimum values corresponding to the smallest particle size and the highest concentration. The reactions have been followed using NMR and GC–MS to determine products and the progress of the reaction. Fig. 2 shows the time course of an experiment with 4-fluorophenol over a 24 h period. In Fig. 2, the peak at −124.8 ppm corresponds to the $^{19}F$ resonance of 4-fluorobenzene and −119.6 ppm is that of fluoride ion in $H_2O$ referenced to $CFCl_3$. This shows the increased production of fluoride ion over the 24 h period with little evidence for catalysis mortality. The conversion observed in 4-fluorophenol of 59.5% corresponds to a [product]:[nanoparticle] ratio of 275. In the case of 4-fluorophenol the other reaction product is 1,4-dihydroxybenzene resulting from an oxidation of the solvent. Table 2 shows a compilation of all the data including quantum yields relative to the oxalate actinometer and turnover numbers based on the production of fluoride ion. Quantum yield (rate of product production/maximum rate of photons absorption) values are difficult to correlate to literature values. We are in the typical range of values seen for other photoreductive dehalogenations on ZnS [9], however we are monitoring only the production of free fluoride from monofluorinated compounds, not step wise photodefluorination of more substituted systems. Fig. 3 shows the time course

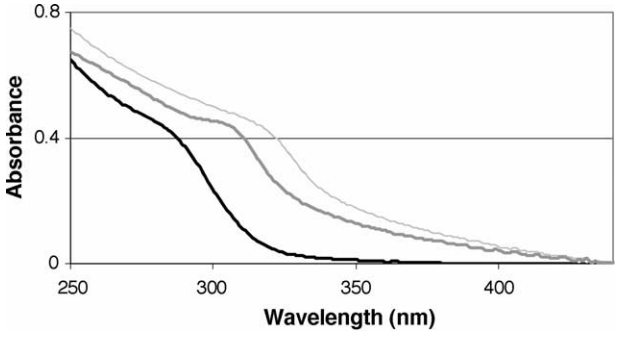


Fig. 1. Absorbance of the ZnS nanoparticles. (Black) freshly prepared 3.6 nm ZnS, (dark gray) 2-day-old 4.4 nm ZnS, (light gray) 4-day-old 6.1 nm ZnS.

Table 1
$^{19}F$ Chemical Shifts (ppm vs. $CFCl_3 = 0.0$) in $H_2O$

| Compound | δF |
|---|---|
| Fluoride (aqueous) | −119.4 |
| 2-Fluorophenol | −137.8 |
| 3-Fluorophenol | −112.7 |
| 4-Fluorophenol | −125.1 |
| 2-Fluorobenzoic acid | −115.4 |
| 3-Fluorobenzoic acid | −113.7 |
| 4-Fluorobenzoic acid | −109.4 |

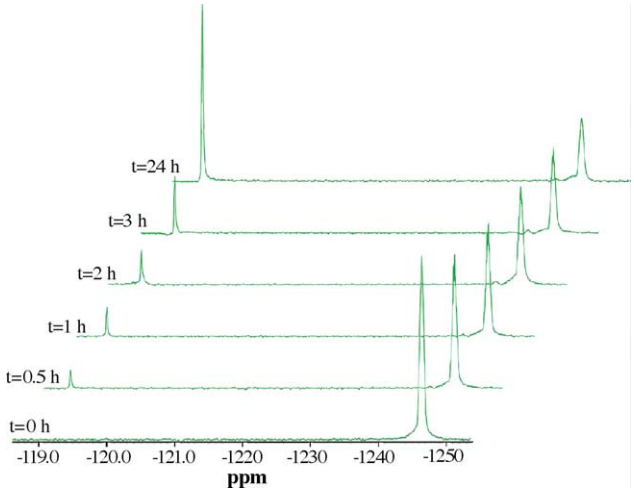


Fig. 2. NMR spectra of 4-fluorophenol photodegradation in the presence of 3.6 nm ZnS at $t = 0$, 0.5, 1, 2, 3 and 24 h.

Table 2
Quantum yield (moles)[a] and turnover number[b] for substrates

| Compound | $\Phi$ | $T/O$ |
|---|---|---|
| Fluoride (aqueous) | | |
| 2-Fluorophenol | 0.08 | 217 |
| 3-Fluorophenol | 0.03 | 81 |
| 4-Fluorophenol | 0.14 | 275 |
| 2-Fluorobenzoic acid | 0.03 | 142 |
| 3-Fluorobenzoic acid | 0.05 | 188 |
| 4-Fluorobenzoic acid | 0.06 | 120 |

[a] Average moles fluoride ion produced/average moles of radiation absorbed.
[b] Average fluoride yield (mM)/catalyst concentration (yields a minimum value).

of fluoride production for the 2-, 3-, and 4-fluorophenol over a 24 h period. The oxidation product of these three reactions is the corresponding 2-, 3-, or 4-dihydroxybenzene. The rates of these photolysis experiments can be considered in the context of the electron donating hydroxyl group. Resonance stabilization effects on the aromatic ring lead to the increased negative charge on the 2 and 4 positions of the ring. This should lead to a lower reduction potential and thus a faster reaction when compared to the 3 position. The increased rate of the 4 versus 2 positions can be accounted for by steric effects. When compared to the fluorobenzoic acid derivatives, the opposite trend should be observed. The electron withdrawing carboxylate group would have the opposite effect on the fluoride substituent and thus the alternate trend should be observed, as is the case in Fig. 4. The products isolated by NMR and GC–MS for the benzoic acid derivatives are fluoride and the corresponding hydroxybenzoic acid or dimethylaminobenzoic acid resulting from the oxidation of the mixed solvent system of water and DMF. Comparison of the rates of reaction for the ortho and para derivatives follows similar arguments, both the 2- and 4-fluorophenol, which experience resonance stabilization through the ring system, is faster than the 2- and 4-flurobenzoic acid derivatives. Conversely, the 3-fluorobenzoic acid, a meta director, is observed to react faster than the 3-fluorophenol. Some fluorinated compounds used in this study have small absorbance spill over

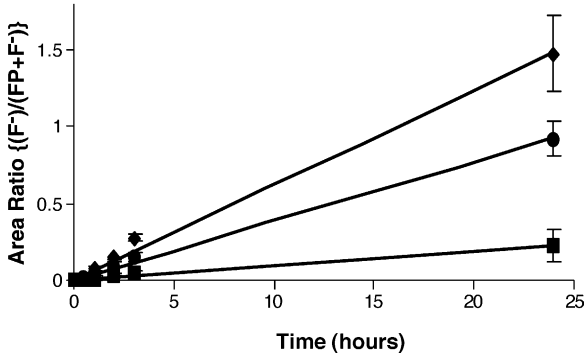


Fig. 3. Increase in fluoride production as a function of irradiation time for the 2- 3-, and 4-fluorophenol systems (circles, squares and diamonds, respectively).

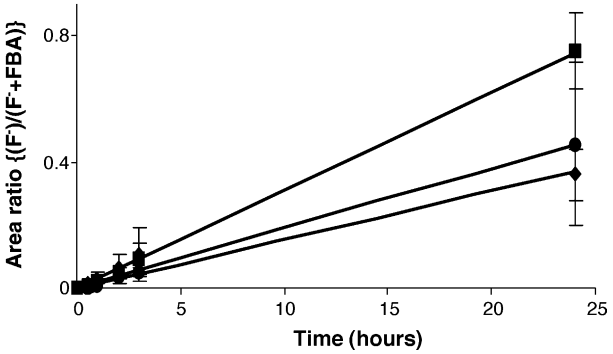


Fig. 4. Increase in fluoride production as a function of irradiation time for the 2- 3-, and 4-fluorobenzoic acid systems (circles, squares and diamonds, respectively).

from 290 to 300 nm. In blank experiments containing each of fluorinated substrates, there is minimal photodegradation without the ZnS nanoparticles present. Significantly less than 1% conversion of starting fluorinated compound in 24 h to unidentified products is observed. In addition, it is worth noting that the products of the "blank" reactions appear to be oxidized compounds, rather than fluoride reduction products. These oxidization products are not observed when the reductive pathway promoted by the presence of ZnS nanoparticles is present.

## 4. Conclusion

The ability of ZnS nanoparticles to defluorinate aromatic compounds under UV irradiation was investigated. The results of this work indicate that 3.6 nm nanoparticles of ZnS can act as an efficient catalyst for the reduction of these compounds to produce inorganic fluoride and the corresponding solvent oxidized aromatic product. The reaction rates are affected by the presence of electron donating or withdrawing groups attached to the aromatic ring and react according to electron donating and withdrawing groups attached to the aromatic ring. The rates of product produced are 4-fluorophenol > 2-fluorophenol > 3-fluorophenol when the electron donating hydroxyl group is present and the opposite trend of 3-fluorobenzoic acid > 2-fluorobenzoic acid > 4-fluorobenzoic acid when an electron withdrawing group is attached to the benzene. Further, when direct comparison of the substituent positions is examined, those substituted in the 2 and 4 positions react further when electron donating groups are present whereas the opposite trend is observed in the 3 position, namely the 3-fluorobenzoic acid is more favorable to undergo fluoride loss than the 3-fluorophenol. Future work includes determining the reactivity of more halogenated aromatics as well as the determination of the effects of dissolved oxygen and pH on nanoparticle assisted photoreduction of halogenated aromatics.

## Acknowledgements

This material is based upon work supported by the National Science Foundation under grant no. 9952343 and 0303994. The authors are grateful to Dr. Chip Detmer, JEOL Inc. for helpful discussions. The authors also thank the College of Arts and Sciences at Armstrong Atlantic State University and the University System of Georgia.

## References

[1] M.R. Hoffmann, S.T. Martin, W. Choi, D.W. Bahnemann, Chem. Rev. 95 (1995) 69–96.
[2] M.A. Fox, M.T. Dulay, Chem. Rev. 93 (1993) 341–357.
[3] A. Mills, A. LeHunte, J. Photochem. Photobiol. A: Chem. 108 (1997) 1–35.
[4] H. Yin, Y. Wada, T. Kitamura, S. Yanagida, Environ. Sci. Technol. 35 (2001) 227–231.
[5] J.P. Wilcoxon, J. Phys. Chem. B 104 (2000) 7334–7343.
[6] D. Shchukin, S. Poznyak, A. Kulak, P. Pichat, J. Photochem. Photobiol. A: Chem. 162 (2004) 423–430.
[7] E. DeFelip, F. Ferri, C. Lupi, N.M. Trieff, F. Volpi, A. diDomenico, Chemosphere 33 (1996) 2263–2271.
[8] C. Kormann, D.W. Bahnemann, M.R. Hoffmann, Environ. Sci. Technol. 25 (1991) 494–500.
[9] Y. Cho, W. Choi, C. Lee, T. Hyeon, H. Lee, Environ. Sci. Technol. 35 (2001) 966–970.
[10] T.R. Thurston, J.P. Wilcoxon, J. Phys. Chem. B. 103 (1999) 11–17.
[11] C.L. Torres-Martinez, R. Kho, O. Mian, R.K. Mehara, J. Colloid Interface Sci. 240 (2001) 525–532.
[12] C.J. Murphy, J.L. Coffer, Appl. Spectrosc. 56 (2002) 16A–21A.
[13] L.E. Brus, J. Chem. Phys. 80 (1984) 4403–4409.
[14] L.E. Brus, J. Phys. Chem. 90 (1986) 2555–2560.
[15] S.G. Joannopoulos, J.D. Kluwer, Photonic Crystals: The Road from Theory to Practice, Johnson, Boston, 2002.
[16] C.B. Murray, C.R. Kagan, M.G. Bawendi, Science 270 (1995) 1335–1338.
[17] V.L. Colvin, M.C. Schlamp, A.P. Alivisatos, Nature 370 (1994) 354–356.
[18] N. Serpone, E. Pelizzetti (Eds.), Photocatalysts—Fundamentals and Applications, Wiley, New York, 1989.
[19] A.A. Khosravi, M. Kundu, L. Jatwa, S.K. Deshpande, U.A. Bhagwat, M. Sastry, S.K. Kulkami, Appl. Phys. Lett. 67 (1995) 2702–2704.
[20] A.P. Alivisatos, J. Phys. Chem. 100 (1996) 13226–13239.
[21] D. Farin, J. Kiwi, D. Avnir, J. Phys. Chem. 93 (1989) 5851–5854.
[22] B.A. Korgel, H.G. Monbouquette, J. Phys. Chem. B 101 (1997) 5010–5017.
[23] G.A. Khitrov, G.F. Strouse, J. Am. Chem. Soc. 125 (2003) 10465–10469.